Int. J. Heat Mass Transfer. Vol. 32, No. 10, pp. 1955–1966, 1989
Printed in Great Britain

0017–9310/89 $3.00 + 0.00
Pergamon Press plc

Some aspects of transient cooling of a radiating rectangular medium

ROBERT SIEGEL
NASA–Lewis Research Center, Office of the Chief Scientist, Cleveland, OH 44135, U.S.A.

(*Received* 6 *October* 1988 *and in final form* 24 *February* 1989)

Abstract—The emission from a gray radiating medium is analyzed for transient cooling in surroundings at a low temperature. The medium is rectangular with no variations in the direction normal to the cross section. The integral equation for the transient temperature distribution is solved numerically using a two-dimensional Gaussian integration subroutine. The emissive ability for a rectangle at uniform temperature is compared with that for transient cooling where the temperature distribution of the region has reached a fully developed shape, as shown by a separation of variables solution. The two solutions provide the upper and lower bounds for the emittance of a rectangle during transient cooling. The emittances for various aspect ratios are presented as a function of the mean length of the rectangle and are compared with results for a plane layer and a cylinder.

INTRODUCTION

THE RADIATIVE behavior of one-dimensional absorbing, emitting, and scattering media, such as planar layers or long cylinders, has received considerable attention in the literature over the past 40 years. The detailed examination of radiative behavior for multi-dimensional geometries is much more recent and has been aided by the availability of increased computing power to solve the integral relations that are involved. The present study is concerned with a rectangular shape; some of the recent radiation analyses for this geometry are given in refs. [1–5]. Most of the investigations in the literature have been for steady conditions, and various solution techniques have been used, such as polynomial approximations [1], finite elements [2], and discrete ordinates [5]. The present study is for transient radiative behavior. The results have applications to the cooling of high temperature porous ceramic insulating materials, and to the energy dissipation by liquid drop or particle heat radiators for elimination of waste heat in outer space. The transient energy equation is a non-linear integral equation for the temperature distribution. It was solved numerically using a two-dimensional Gaussian integration subroutine. The integrations were carried out in regions surrounding node points that were on a square grid of points in the rectangular region. Cubic spline interpolation was used to obtain temperature values between the nodes as required by the integration routine. The method of integration used to avoid any singular numerical behavior will be described.

The radiating medium considered here is initially at uniform temperature and is then placed in low temperature surroundings. It will begin to cool at uniform temperature, and the outer regions will cool most rapidly, yielding transient temperature distributions such as those in ref. [6] for a plane layer. It was found in ref. [6] that after a period of time, the temperature distribution developed a shape that it then retained throughout the remainder of the transient. During this remaining portion of the transient, the emittance became constant. It was also found that the initial emittance for the region at uniform temperature, and the final transient emittance, are bounding values for the entire transient. These bounds show how significant the transient conditions are in influencing the instantaneous heat loss. The fully developed transient region was examined in more detail for a plane layer in ref. [7] by a separation of variables solution. This type of solution can also be applied for non-planar geometries and is used here to examine a rectangular region. The method is applied here to an absorbing–emitting medium, but it can be extended to include scattering. This will be done in a subsequent paper.

The similarity formulation yields a two-dimensional non-linear integral equation for the universal shape of the transient temperature distribution that is ultimately achieved during cooling. The integral equation was solved by iteration, using two-dimensional Gaussian integration subroutines to evaluate the radiative flux integrals. After the temperature distribution was found, the local heat fluxes were evaluated around the rectangular boundary. This reveals the relatively low radiative dissipation at the corners, and how the heat loss at the center of the long side approaches that for a flat layer as the aspect ratio is increased.

ANALYSIS

Energy relations for radiative cooling

The rectangular region shown in Fig. 1(a) is filled with a gray emitting, absorbing, and non-scattering

NOMENCLATURE

A	area of boundary
A_R	aspect ratio of rectangular region, d/b
a	absorption coefficient of radiating medium
B_o	optical length of small side of rectangle, ab
b	length of small side of rectangle
c_p	specific heat of radiating medium
d	length of large side of rectangle
F	function of X, Y in temperature distribution
$\bar{i}$	average radiation intensity
Q	heat loss per unit of length z
q_ℓ	local heat loss along boundary per unit area and time
q_r	radiative heat flow per unit area and time
q_x, q_y	surface heat fluxes in x- and y-directions
R	dimensionless distance between two points
r	position coordinate
S_n	function defined in equation (4)
T	absolute temperature; $\tilde{T} = T/T_i$
T_i	reference temperature or initial temperature
T_P	temperature at center of long side of rectangle
t	intermediate variable used in equation (4)
V	volume
x, y, z	rectangular coordinates; $X = x/b$, $Y = y/b$, $Z = z/b$.

Greek symbols

ε	emittance
ε_{fd}	emittance for fully developed transient conditions based on T_m
ε_{ut}	emittance for region at uniform temperature
ζ, ξ	intermediate variables used to obtain equation (5)
θ	angular coordinate
ρ	density of radiating medium
σ	Stefan–Boltzmann constant
τ	time; $\tilde{\tau} = (4\sigma T_i^3/\rho c_p b)\tau$.

Subscripts

fd	fully developed transient conditions
ℓ	local value along boundary
m	integrated mean value
ut	value for rectangle at uniform temperature.

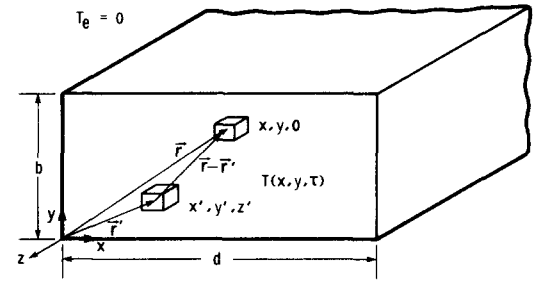

(a)

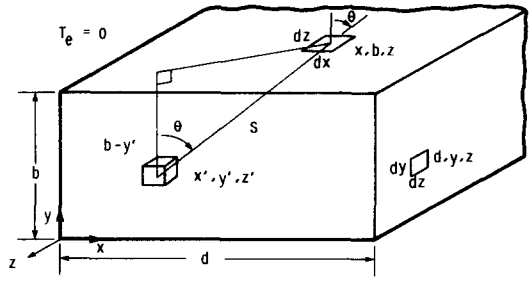

(b)

FIG. 1. Geometry of radiating rectangular region: (a) exchange between interior volume elements; (b) exchange between volume and surface element.

medium. The geometry is long in the z-direction, and the temperature distribution $T(x, y)$ within the medium is independent of z. The surroundings are at a temperature T_e that is low compared with that in the medium, and incident energy from the surroundings is neglected. The medium is initially at a uniform temperature T_i, and some aspects of the transient radiative cooling are to be studied. The local transient cooling depends on the divergence of the radiative flux, and the energy equation has the following form from ref. [8]:

$$\rho c_p \frac{\partial T}{\partial \tau} = -\nabla \cdot \mathbf{q}_r. \tag{1}$$

The flux divergence is the difference between the local emitted energy and the energy absorbed from the incident intensity arising from emission by all of the surrounding volume elements [8]

$$\nabla \cdot \mathbf{q}_r = 4a(\sigma T^4 - \pi \bar{i}) \tag{2}$$

where

$$\bar{i} = \frac{a}{4\pi} \int_V \frac{\sigma T^4(\mathbf{r}')}{\pi} \frac{e^{-a|\mathbf{r}-\mathbf{r}'|}}{|\mathbf{r}-\mathbf{r}'|^2} dV.$$

Combining equations (1) and (2) yields an integral equation for the transient temperature distribution

$$-\rho c_p \frac{\partial T}{\partial \tau} = 4a\sigma T^4 - \frac{a^2}{\pi}\int_V \sigma T^4(\mathbf{r}')\frac{e^{-a|\mathbf{r}-\mathbf{r}'|}}{|\mathbf{r}-\mathbf{r}'|^2}\,dV. \quad (3)$$

The volume integral in equation (3) is written as

$$2\int_{x'=0}^{d}\int_{y'=0}^{b}\sigma T^4(x', y')\int_{z'=0}^{\infty} \times \frac{\exp\{-a[(x-x')^2+(y-y')^2+z'^2]^{1/2}\}}{(x-x')^2+(y-y')^2+z'^2}\,dz'\,dx'\,dy'.$$

Letting

$$\xi' = z'/[(x-x')^2+(y-y')^2]^{1/2} \equiv z'/\zeta'$$

and

$$t = (1+\xi'^2)^{1/2}$$

the volume integral becomes

$$2\int_{x'=0}^{d}\int_{y'=0}^{b}\sigma T^4(x', y')\frac{\pi}{2}\frac{S_1(a\zeta')}{\zeta'}\,dx'\,dy'$$

where S_1 is one of the class of functions

$$S_n(x) = \frac{2}{\pi}\int_1^{\infty}\frac{e^{-xt}}{t^n(t^2-1)^{1/2}}\,dt = \frac{2}{\pi}\int_0^{\pi/2} e^{-x/(\cos\theta)}\cos^{n-1}\theta\,d\theta. \quad (4)$$

The S_n functions arise in two-dimensional radiative transfer, and their behavior was examined in detail in ref. [9]. The energy equation then has the form

$$-\frac{\rho c_p}{a}\frac{\partial T}{\partial \tau} = 4\sigma T^4 - a^2\int_{x'=0}^{d}\int_{y'=0}^{b}\sigma T^4(x', y', \tau)\frac{S_1(a\zeta')}{a\zeta'}\,dx'\,dy'. \quad (5)$$

Utilizing the dimensionless groups in the Nomenclature, this becomes

$$-\frac{1}{B_o}\frac{\partial \tilde{T}}{\partial \tilde{\tau}} = \tilde{T}^4(X, Y, \tilde{\tau}) - \frac{B_o}{4}\int_{X'=0}^{A_R}\int_{Y'=0}^{1}\tilde{T}^4(X', Y', \tilde{\tau})\frac{S_1(B_oR)}{R(X, Y, X', Y')}\,dX'\,dY' \quad (6)$$

where

$$R(X, Y, X', Y') = [(X'-X)^2+(Y'-Y)^2]^{1/2}.$$

This is a non-linear integral equation for the transient temperature distribution.

The transient solution for a radiating plane layer [6], which was initially at uniform temperature, showed that the transient emittance is highest at the start of the cooling when the outer portions of the radiating region have not yet cooled more than the interior. As cooling proceeds, the outer regions are at lower temperatures, which reduces the radiative ability of the region. It was found numerically that the emittance based on the instantaneous mean temperature and average boundary heat flux decreases from its initial value ε_{ut} for a uniform temperature region, to a lower value $\varepsilon_{fd} = q(\tilde{\tau})/\sigma T_m^4(\tilde{\tau})$ when the transient temperature distribution has reached a 'fully developed' shape. For this fully developed transient temperature distribution, which satisfies the energy equation (equation (6)) the instantaneous heat loss is in a fixed proportion to the fourth power of the instantaneous mean temperature. Thus ε_{ut} and ε_{fd} provide upper and lower bounds for the situation of transient radiative cooling in low temperature surroundings. These bounds will be examined here for a rectangular region.

Separable solution

A solution for equation (6) is tried in the form

$$\tilde{T}(X, Y, \tilde{\tau}) = \tilde{T}\left(\frac{A_R}{2}, 0, \tilde{\tau}\right)F(X, Y) = \tilde{T}_P(\tilde{\tau})F(X, Y). \quad (7)$$

Since $\tilde{T}_P$ is defined as the value of $\tilde{T}$ at the center of the long side, $X = A_R/2$, $Y = 0$, the $F(A_R/2, 0)$ is arbitrarily fixed at unity. $F(X, Y)$ is the two-dimensional shape of the temperature distribution, and $\tilde{T}_P(\tilde{\tau})$ shows how the temperatures are decreasing with time. Substituting equation (7) into equation (6) yields

$$\frac{1}{\tilde{T}_P^4(\tilde{\tau})}\frac{d\tilde{T}_P}{d\tilde{\tau}} = -\frac{B_o}{F(X, Y)}\left[F^4(X, Y) - \frac{B_o}{4}\int_{X'=0}^{A_R}\int_{Y'=0}^{1}F^4(X', Y')\frac{S_1(B_oR)}{R}\,dX'\,dY'\right]. \quad (8)$$

Since the variables have been separated ($\tilde{\tau}$ on the left and X, Y on the right) each side of equation (8) must be a constant. Then to obtain an equation for $F(X, Y)$, the left-hand side of equation (8) is equated to itself at any convenient value of X, Y; $X = A_R/2$, $Y = 0$ was used because $F(A_R/2, 0) = 1$. This results in an integral equation for $F(X, Y)$

$$F^4(X, Y) = F(X, Y)\left\{1 - \frac{B_o}{4}\int_{X'=0}^{A_R}\int_{Y'=0}^{1}F^4(X', Y') \times \frac{S_1\left[B_oR\left(\frac{A_R}{2}, 0, X', Y'\right)\right]}{R\left(\frac{A_R}{2}, 0, X', Y'\right)}\,dX'\,dY'\right\} + \frac{B_o}{4}\int_{X'=0}^{A_R}\int_{Y'=0}^{1}F^4(X', Y') \times \frac{S_1[B_oR(X, Y, X', Y')]}{R(X, Y, X', Y')}\,dX'\,dY'. \quad (9)$$

Average and local emittance relations

The emittance in the fully developed transient

region can be found from a heat balance for the entire rectangle

$$2\varepsilon_{fd}(b+d)\sigma T_m^4 = -\rho c_p bd\frac{dT_m(\tau)}{d\tau} \quad (10a)$$

which yields in dimensionless form

$$\varepsilon_{fd} = -\frac{2A_R}{1+A_R}\frac{1}{\tilde{T}_m^4}\frac{d\tilde{T}_m}{d\tilde{\tau}}. \quad (10b)$$

From its definition, the mean temperature of the radiating medium is

$$T_m(\tau) = \frac{1}{bd}\int_{y=0}^{b}\int_{x=0}^{d} T(x, y, \tau)\,dx\,dy \quad (11a)$$

which has the dimensionless form

$$\tilde{T}_m(\tilde{\tau}) = \frac{1}{A_R}\int_{X=0}^{A_R}\int_{Y=0}^{1}\tilde{T}(X, Y, \tilde{\tau})\,dX\,dY. \quad (11b)$$

Using equation (7) expresses $\tilde{T}_m$ in terms of $\tilde{T}_P(\tilde{\tau})$ and F_m as

$$\tilde{T}_m(\tilde{\tau}) = \tilde{T}_P(\tilde{\tau})\frac{1}{A_R}\int_{X=0}^{A_R}\int_{Y=0}^{1}F(X, Y)\,dX\,dY$$

$$= \tilde{T}_P(\tilde{\tau})F_m. \quad (12)$$

Then from equation (10b)

$$\varepsilon_{fd} = -\frac{2A_R}{1+A_R}\frac{1}{F_m^3}\left(\frac{1}{\tilde{T}_P^4}\frac{d\tilde{T}_P}{d\tilde{\tau}}\right). \quad (13a)$$

The quantity in parentheses on the right-hand side of equation (13a) is a constant. This can be found from the right-hand side of equation (8) yielding ε_{fd} in terms of the solution for $F(X, Y)$, where for convenience the relation has been evaluated at the center of the long side

$$\varepsilon_{fd} = \frac{2A_R}{1+A_R}\frac{B_o}{F_m^3}\left\{1-\frac{B_o}{4}\int_{X'=0}^{A_R}\int_{Y'=0}^{1}F^4(X', Y')\right.$$

$$\left.\times\frac{S_1\left[B_oR\left(\frac{A_R}{2}, 0, X', Y'\right)\right]}{R\left(\frac{A_R}{2}, 0, X', Y'\right)}dX'\,dY'\right\}. \quad (13b)$$

Equation (13b) provides the emittance of the rectangular region so that in the fully developed transient region the instantaneous heat loss per unit of length z is $Q_{fd}(\tau) = 2(b+d)\varepsilon_{fd}\sigma T_m^4(\tau)$.

The result in equation (13b) does not give any information about the distribution of radiative energy loss from locations around the boundary of the rectangle. This can be found by obtaining local radiative flux relations. Referring to Fig. 1(b), the energy $a\sigma T^4(x', y', z')\,dV'/\pi$ is emitted from dV' per unit solid angle. This is attenuated by the factor e^{-aS} before reaching the surface element at x, b, z. Since $\cos\theta = (b-y')/S$, the solid angle that element $dx\,dz$ subtends when viewed from x', y', z' is $dx\,dz(b-y')/S^3$. Then to obtain the energy flux radiated through $dx\,dz$ from all volume elements, integrate over all x', y', z' to obtain

$$q_y(x, \tau) = \frac{2a}{\pi}\int_{x'=0}^{d}\int_{y'=0}^{b}\sigma T^4(x', y', \tau)$$

$$\times\int_{z'=0}^{\infty}\frac{(b-y')\exp\{-a[(x-x')^2+(b-y')^2+z'^2]^{1/2}\}}{[(x-x')^2+(b-y')^2+z'^2]^{3/2}}$$

$$\times dz'\,dx'\,dy'. \quad (14)$$

By using the same transformations as used to obtain equation (5), q_y is expressed in terms of the function S_2 to yield

$$q_y(x, \tau) = a\int_{x'=0}^{d}\int_{y'=0}^{b}$$

$$\times\sigma T^4(x', y', \tau)(b-y')\frac{S_2(ar_2)}{r_2^2}dx'\,dy' \quad (15)$$

where

$$r_2 = [(x-x')^2+(b-y')^2]^{1/2}.$$

$q_x(y, \tau)$ is similarly derived, and the fluxes are placed in dimensionless form to yield

$$\frac{q_y(X, \tilde{\tau})}{\sigma T_i^4} = B_o\int_{X'=0}^{A_R}\int_{Y'=0}^{1}\tilde{T}^4(X', Y', \tilde{\tau})(1-Y')$$

$$\times\frac{S_2(B_oR_2)}{R_2^2}dX'\,dY' \quad (16a)$$

$$\frac{q_x(Y, \tilde{\tau})}{\sigma T_i^4} = B_o\int_{X'=0}^{A_R}\int_{Y'=0}^{1}\tilde{T}^4(X', Y', \tilde{\tau})(A_R-X')$$

$$\times\frac{S_2(B_oR_1)}{R_1^2}dX'\,dY' \quad (16b)$$

where

$$R_2^2 = (X-X')^2+(1-Y')^2$$

$$R_1^2 = (A_R-X')^2+(Y-Y')^2.$$

For a rectangle at uniform temperature $T = T_i$, the $\tilde{T} = 1$ and equations (16a) and (16b) yield the local emittance values

$$\varepsilon_{ut}(X) = \frac{q_y(x)}{\sigma T_i^4}$$

$$= B_o\int_{X'=0}^{A_R}\int_{Y'=0}^{1}S_2(B_oR_2)\frac{1-Y'}{R_2^2}dX'\,dY' \quad (17a)$$

$$\varepsilon_{ut}(Y) = \frac{q_x(y)}{\sigma T_i^4}$$

$$= B_o \int_{X'=0}^{A_R} \int_{Y'=0}^{1} S_2(B_o R_1) \frac{A_R - X'}{R_1^2} dX' dY'. \quad (17b)$$

For fully developed transient conditions, the emittance was based on the instantaneous mean temperature of the region. Then equation (7) is used, and by use of equations (16a) and (16b), the emittances become

$$\varepsilon_{fd}(X) = \frac{q_y(x,\tau)}{\sigma T_m^4(\tau)}$$

$$= \frac{B_o}{F_m^4} \int_{X'=0}^{A_R} \int_{Y'=0}^{1} F^4(X', Y') S_2(B_o R_2) \times \frac{1 - Y'}{R_2^2} dX' dY' \quad (18a)$$

$$\varepsilon_{fd}(Y) = \frac{q_x(y,\tau)}{\sigma T_m^4(\tau)}$$

$$= \frac{B_o}{F_m^4} \int_{X'=0}^{A_R} \int_{Y'=0}^{1} F^4(X', Y') S_2(B_o R_1) \times \frac{A_R - X'}{R_1^2} dX' dY'. \quad (18b)$$

By integrating ε around the boundary and obtaining an area weighted average, ε_{ut} or ε_{fd} is obtained for the rectangle as

$$\varepsilon = \frac{1}{1 + A_R} \left[\int_{X=0}^{A_R} \varepsilon(X) dX + \int_{Y=0}^{1} \varepsilon(Y) dY \right] \quad (19)$$

where ε is either ε_{ut} or ε_{fd}. The corresponding heat losses per unit length in the z-direction are $Q_{ut} = 2(b+d)\varepsilon_{ut}\sigma T_i^4$ and $Q_{fd}(\tau) = 2(b+d)\varepsilon_{fd}\sigma T_m^4(\tau)$.

Note that ε_{ut} is based on the uniform temperature T_i of the region. The local and mean values of ε_{fd} were based on the instantaneous mean temperature $T_m(\tau)$ from equation (11a). For the transient situation, local ε values along the boundary could also be defined by using the local heat loss and local temperature along the boundary. Using equation (18), these values are (the subscript ℓ indicates ε is based on the local boundary temperature

$$\varepsilon_{fd,\ell}(X) = \frac{q_y(x,\tau)}{\sigma T^4(x,b,\tau)} = \left[\frac{F_m}{F(X,1)} \right]^4 \varepsilon_{fd}(X) \quad (20a)$$

$$\varepsilon_{fd,\ell}(Y) = \frac{q_x(y,\tau)}{\sigma T^4(d,y,\tau)} = \left[\frac{F_m}{F(Y,A_R)} \right]^4 \varepsilon_{fd}(Y). \quad (20b)$$

The mean beam length for an optically thin region, $L_{e,o}$, is used as a characteristic length for the comparison of values of ε for various geometries. From ref. [8] $L_{e,o} = 4V/A$ so for a cylinder of diameter D, $L_{e,o} = D$; for a plane layer of thickness, D, $L_{e,o} = 2D$; and for a rectangle

$$L_{e,o} = \frac{2bd}{b+d} \quad \text{or} \quad aL_{e,o} = \frac{2B_o A_R}{A_R + 1}. \quad (21)$$

Numerical solution

The integral equation (equation (9)) was solved numerically by iteration, starting with $F(X, Y) = 1$ as an initial function. The solution was carried out for several optical lengths, B_o, and three aspect ratios, A_R. The initial $F(X, Y)$ was substituted into the right-hand side. After carrying out the double integration, the difference between the right-hand side and the trial $F^4(X, Y)$ was multiplied by an acceleration factor 1.5, and the result added to the trial $F^4(X, Y)$ to obtain a new $F^4(X, Y)$. This was inserted into the right-hand side of equation (9) to continue the iteration. Usually about 15 iterations were required to obtain convergence to where the change in F^4 at any X, Y relative to the F^4 at that location was less than 10^{-4}. Most cases required about 25 min running time on an IBM 370 computer.

From symmetry it is only necessary to solve for values in one quadrant, as shown in Fig. 2(a). The values at the grid points are then transferred to the other quadrants so that the double integrations can be carried out to include the entire area of the rectangle. The quadrant in Fig. 2(a) was covered with equally spaced grid points on a square grid; a typical grid point is at x, y on the figure. Across the short side of the rectangle, either 15, 20, 30, or 40 increments were used. Test cases showed that 20 or 30 increments usually gave accurate results. To carry out the integrations, two-dimensional spline fits were made of $F(X, Y)$ using the IMSL routine CSINT. The geometry was usually divided into subregions to improve the

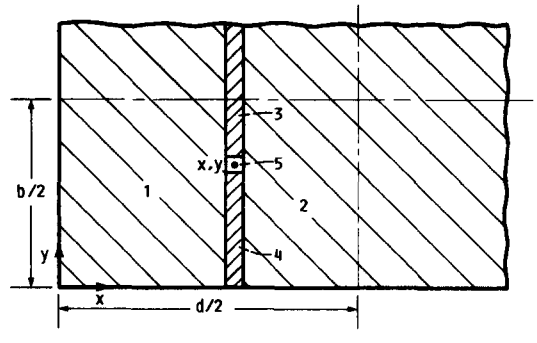

(a)

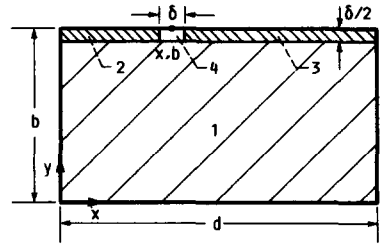

(b)

FIG. 2. Integration regions for solving radiative transfer relations: (a) regions for solution of energy equation; (b) regions for obtaining surface heat fluxes.

curve fit accuracy. The spline coefficients were then used to interpolate values at locations between the grid points for use in a two-dimensional Gaussian integration subroutine (IMSL routine QAND). The subroutine required irregularly spaced points throughout the integration region surrounding each grid point. The number of Gaussian integration points in each coordinate direction was usually several times the number of grid points. Other solution techniques could be used such as in refs. [1, 2, 5], but the present method should yield an 'exact' solution if the integrations are done carefully.

A numerical difficulty with equation (9) is that the last term appears to have a singularity in the kernel as X', Y' approaches X, Y so that R approaches zero. Actually, the integrand is not singular, as shown by using cylindrical coordinates. In cylindrical coordinates $dX'\,dY'$ becomes $R\,dR\,d\theta$, and the R is thus removed from the denominator. To avoid numerical difficulties, the integration was carried out in cylindrical coordinates for a small region, area 5 in Fig. 2(a), surrounding the grid point. The remainder of the integration was carried out using rectangular coordinates over the rectangular regions 1–4 in Fig. 2(a). The width of shaded strips 3 and 4 was less than one grid spacing.

A similar procedure was used to evaluate the integrals in equation (18) for the surface heat flux distributions. The integrands are again nonsingular, as is evident in cylindrical coordinates. Three rectangular regions were used, 1–3 as shown in Fig. 2(b), and cylindrical coordinates were used to integrate over the small region 4 surrounding the boundary grid point. The size of δ in Fig. 2(b) was less than one grid spacing.

RESULTS AND DISCUSSION

As described in the numerical section, the integral equation (equation (9)) was solved by iteration for $F(X, Y)$. This is the fully developed shape achieved by the temperature distribution during transient radiative cooling in surroundings that are at a much lower temperature. The transient temperature distribution has been normalized by its transient value at the center of the long boundary, $x = d/2$, $y = 0$, and the ratio, $F(x, y) = T(x, y, \tau)/T(d/2, 0, \tau)$ is independent of time. This is the temperature distribution that will be reached during transient cooling, and it depends on the aspect ratio, d/b, of the rectangle and on the optical length of the short side, ab.

The shapes of typical fully developed temperature profiles are shown in Fig. 3, and according to their normalization, they pass through unity at $x/d = 0.5$ and $y/b = 0$. Figure 3(a) is for an aspect ratio of 2 and shows the effect of the optical dimension for $ab = 2$ and 6. This range of ab was chosen on the basis of previous work in refs. [6, 10]. For $ab < 2$ the region becomes somewhat optically thin and the temperature

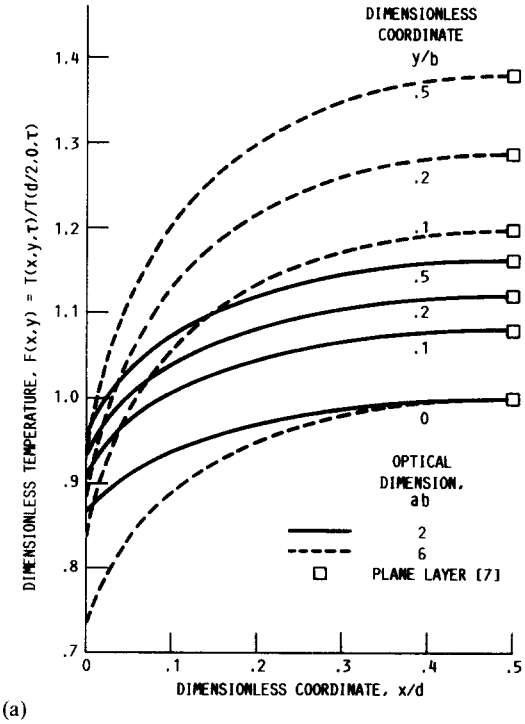

(a)

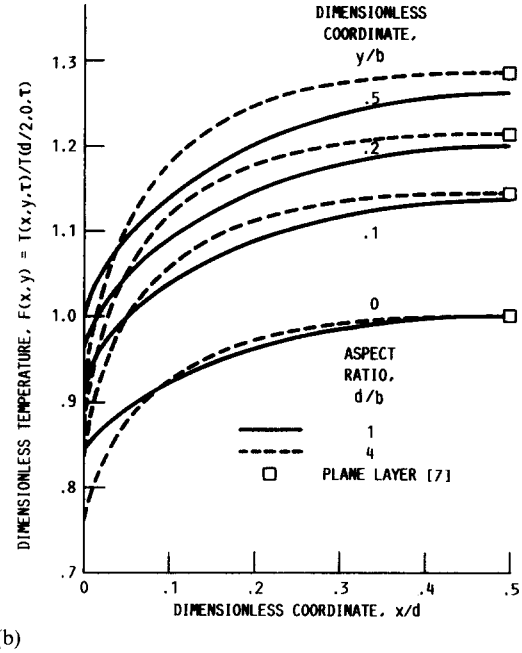

(b)

FIG. 3. Temperature distributions for fully developed transient cooling of a rectangular region: (a) aspect ratio, $d/b = 2$; (b) optical dimension, $ab = 4$.

distributions are rather flat. An $ab = 6$ shows the behavior for a rather optically thick region. As would be expected, the temperatures are highest in the center of the rectangle, and they decrease at an increasing rate in the heat flow directions toward the boundaries. The lowest temperature is at the corner. An increase

in optical thickness does not alter the general form of the distribution, but considerably increases the amplitude from the corner of the rectangle to the center. Figure 3(b) shows profiles for an optical dimension $ab = 4$, and for two aspect ratios, a square, and a long rectangle, $d/b = 4$. The increase of aspect ratio raises the amplitude of the distribution and provides a more uniform distribution along the x-direction in the central portion of the long dimension. From the study in ref. [7] the temperature results are shown in Fig. 3 for transient cooling of plane layers with optical thicknesses 2, 4, and 6. For the rectangle with aspect ratio 4 in Fig. 3(b), the temperature profile in the y-direction, across the center of the long dimension, agrees with that for a plane layer. This is also shown to be true in Fig. 3(a) for an aspect ratio of 2 and for optical thicknesses of the short side of 2 and 6.

The rectangle is initially at a uniform temperature T_i. For this condition, the local heat fluxes leaving the boundaries were evaluated from equations (17a) and (17b) and were normalized by σT_i^4 to give the local emittance variations. These are given in Table 1, and some of the values are shown in Fig. 4. In Fig. 4(a), the optical length of the short side is 2, and results are given for three aspect ratios 1, 2, and 4. The smallest local emittance is at the corner, which can be thought of as a locally optically thin region. The emittance increases away from the corner and reaches its maximum at the center of the long side. The curves for $d/b = 4$ practically coincide with those for $d/b = 2$, and along the long side, the emittance reaches the value for a plane layer with an optical thickness equal to ab. A further increase in aspect ratio would not change the behavior in the end regions and would add boundary area having the same emittance as for a plane layer as given in ref. [6]. This behavior is more pronounced when the optical density of the rectangle is increased, as in Fig. 4(b), where ab is twice that in Fig. 4(a). The local emittance for an aspect ratio of 4 follows that for $d/b = 1$ and rapidly reaches the value for a plane layer. For large optical density, there is a small end region of low emittance adjacent to the

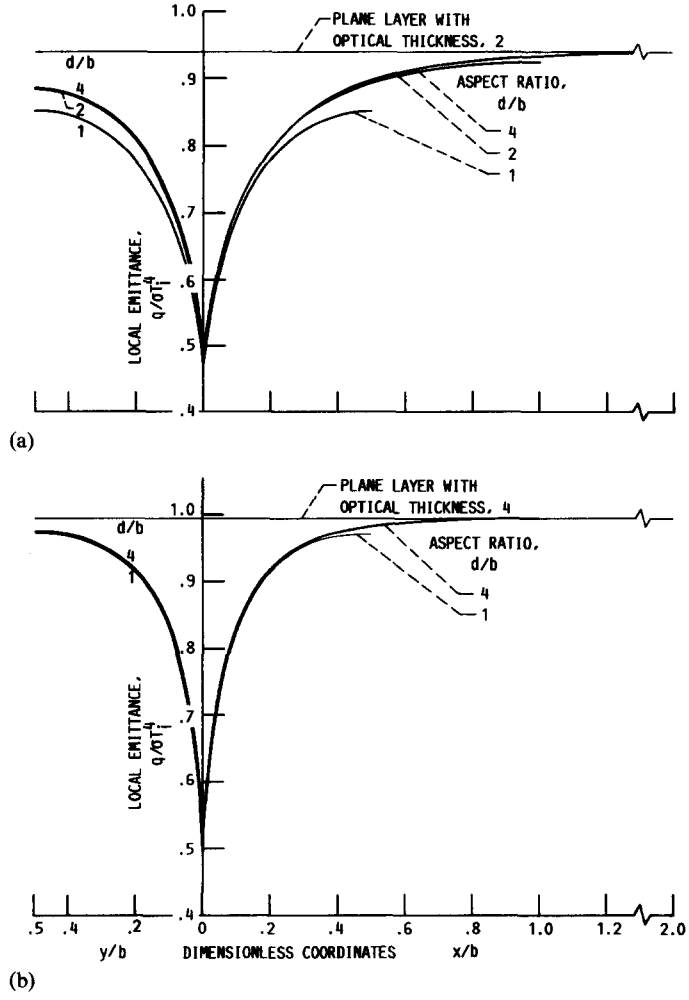

FIG. 4. Local emittance along boundary for radiating rectangular region at uniform temperature (plane layer results from ref. [6]): (a) optical dimension, $ab = 2$; (b) optical dimension, $ab = 4$.

Table 1. Local emittance values along sides of rectangular region

($\varepsilon_{ut} = q_r/\sigma T_i^4$, $\varepsilon_{fd} = q_r/\sigma T_m^4$)

(a) Aspect ratio, $d/b = 1$

	Optical dimension, ab							
	1		2		4		6	
x/b or y/b	ε_{ut}	ε_{fd}	ε_{ut}	ε_{fd}	ε_{ut}	ε_{fd}	ε_{ut}	ε_{fd}
0	0.369	0.351	0.462	0.405	0.496	0.341	0.500	0.262
0.1	0.513	0.492	0.693	0.619	0.827	0.612	0.882	0.540
0.2	0.575	0.567	0.779	0.738	0.913	0.773	0.957	0.709
0.3	0.611	0.613	0.823	0.815	0.950	0.877	0.982	0.820
0.4	0.631	0.639	0.845	0.858	0.966	0.937	0.991	0.885
0.5	0.636	0.648	0.852	0.872	0.970	0.957	0.993	0.906

(b) Aspect ratio, $d/b = 2$

	Optical dimension, ab							
	1		2		4		6	
x/b	ε_{ut}	ε_{fd}	ε_{ut}	ε_{fd}	ε_{ut}	ε_{fd}	ε_{ut}	ε_{fd}
0	0.387	0.348	0.469	0.363	0.497	0.272	0.500	0.193
0.1	0.537	0.484	0.703	0.554	0.828	0.490	0.885	0.402
0.2	0.605	0.564	0.793	0.674	0.916	0.635	0.957	0.544
0.3	0.649	0.625	0.843	0.764	0.955	0.740	0.982	0.653
0.4	0.680	0.672	0.874	0.835	0.973	0.826	0.992	0.739
0.5	0.700	0.709	0.894	0.889	0.982	0.895	0.996	0.805
0.6	0.715	0.733	0.907	0.931	0.987	0.945	0.997	0.855
0.7	0.725	0.753	0.915	0.962	0.990	0.982	0.998	0.892
0.8	0.732	0.768	0.920	0.984	0.991	1.008	0.998	0.917
0.9	0.735	0.776	0.923	0.996	0.992	1.023	0.999	0.931
1.0	0.737	0.779	0.924	1.000	0.992	1.028	0.999	0.936

	Optical dimension, ab							
	1		2		4		6	
y/b	ε_{ut}	ε_{fd}	ε_{ut}	ε_{fd}	ε_{ut}	ε_{fd}	ε_{ut}	ε_{fd}
0	0.426	0.396	0.485	0.391	0.499	0.280	0.500	0.196
0.1	0.575	0.531	0.719	0.579	0.827	0.495	0.884	0.403
0.2	0.641	0.605	0.806	0.689	0.916	0.628	0.957	0.535
0.3	0.678	0.652	0.852	0.761	0.953	0.715	0.982	0.624
0.4	0.698	0.680	0.875	0.802	0.969	0.767	0.991	0.677
0.5	0.705	0.689	0.882	0.815	0.974	0.784	0.993	0.694

(c) Aspect ratio, $d/b = 4$

	Optical dimension, ab							
	1		2		4		6	
x/b	ε_{ut}	ε_{fd}	ε_{ut}	ε_{fd}	ε_{ut}	ε_{fd}	ε_{ut}	ε_{fd}
0	0.390	0.320	0.470	0.314	0.497	0.224	0.500	0.159
0.2	0.609	0.520	0.794	0.586	0.916	0.523	0.957	0.446
0.4	0.685	0.625	0.875	0.734	0.973	0.691	0.992	0.607
0.6	0.724	0.695	0.908	0.832	0.987	0.801	0.997	0.708
0.8	0.745	0.743	0.924	0.900	0.991	0.874	0.998	0.773
1.0	0.758	0.778	0.932	0.947	0.993	0.923	0.998	0.815
1.2	0.767	0.803	0.935	0.981	0.994	0.956	0.998	0.846
1.4	0.770	0.818	0.937	1.000	0.994	0.974	0.998	0.856
1.6	0.771	0.828	0.938	1.011	0.994	0.982	0.999	0.860
1.8	0.772	0.833	0.939	1.018	0.994	0.987	0.999	0.862
2.0	0.772	0.835	0.939	1.020	0.994	0.988	0.999	0.863

	Optical dimension, ab							
	1		2		4		6	
y/b	ε_{ut}	ε_{fd}	ε_{ut}	ε_{fd}	ε_{ut}	ε_{fd}	ε_{ut}	ε_{fd}
0	0.441	0.384	0.487	0.344	0.499	0.231	0.500	0.161
0.1	0.589	0.506	0.721	0.507	0.828	0.409	0.885	0.331
0.2	0.656	0.575	0.808	0.603	0.917	0.518	0.957	0.438
0.3	0.695	0.619	0.854	0.666	0.954	0.592	0.982	0.511
0.4	0.715	0.637	0.877	0.702	0.969	0.635	0.991	0.553
0.5	0.722	0.645	0.884	0.714	0.974	0.649	0.993	0.567

short side, and the remainder of the rectangle has a local emittance equal to that for a plane layer.

As the rectangle continues to cool, the fully developed temperature profiles are reached as determined by the separation of variables solution in the analysis. T_m^4 is found to decrease with time at the same rate as the local heat loss is decreasing so that the local emittance along the boundary is not a function of time. The mean temperature, T_m, can be greater or less than the local temperatures in the medium near the boundaries, which are the most significant temperatures in providing the local heat loss, unless the region is optically thin. The ratio of local $q_\ell/\sigma T_m^4$ along the boundaries can thus exceed unity and cannot be regarded in terms of the usual emittance definition. The emittance of a radiating medium is only properly defined if the medium has a uniform temperature and composition. The lower temperatures in the end regions of the rectangle decrease the mean temperature of the entire region, and hence cause the ratio $q_\ell/\sigma T_m^4$ to be high in the central portion of the long boundary. Table 1 and Figs. 5(a) and (b) give

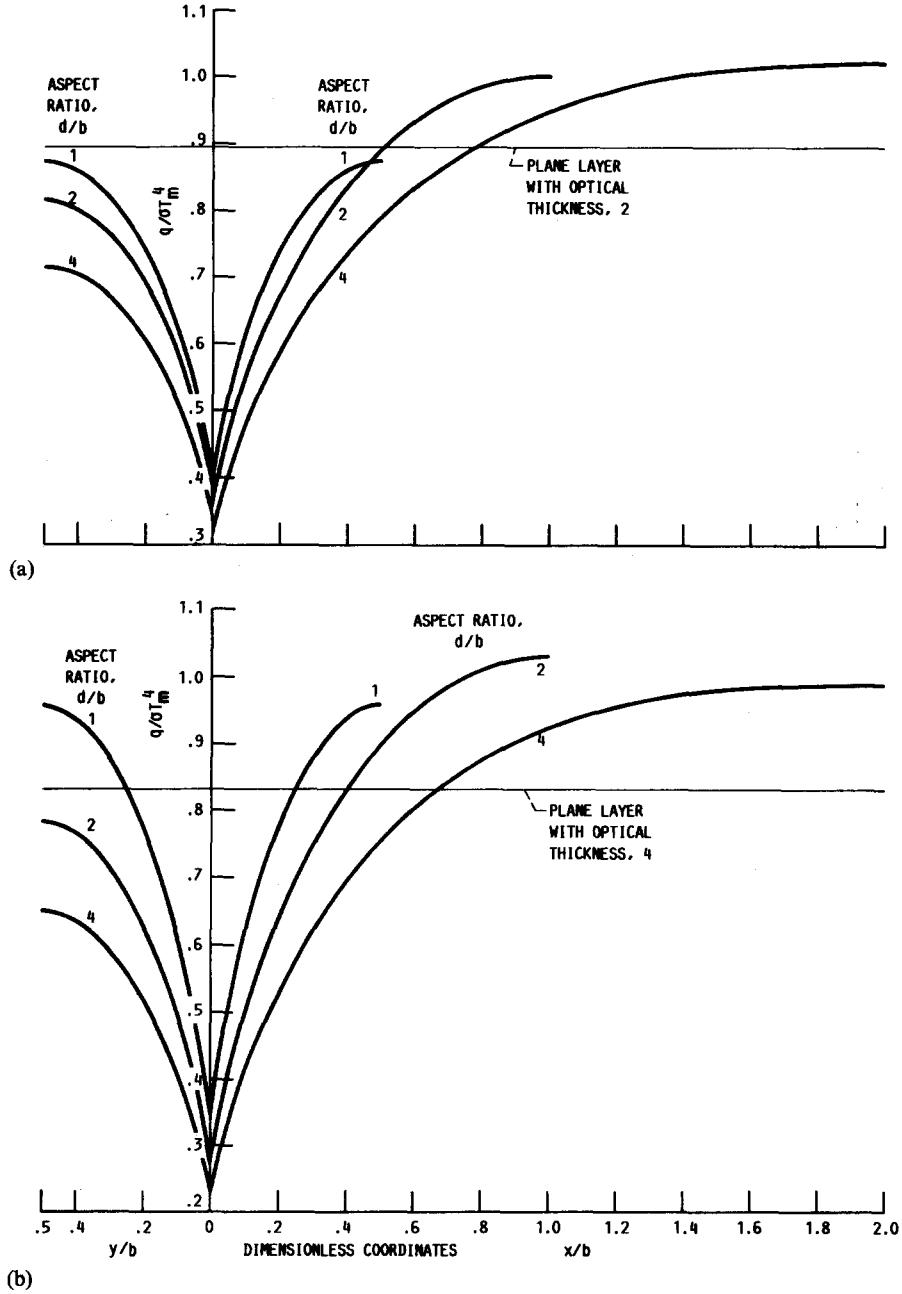

FIG. 5. Local emittance along boundary for fully developed transient cooling; emittance is based on mean temperature of region (plane layer results from ref. [7]): (a) optical dimension, $ab = 2$; (b) optical dimension, $ab = 4$.

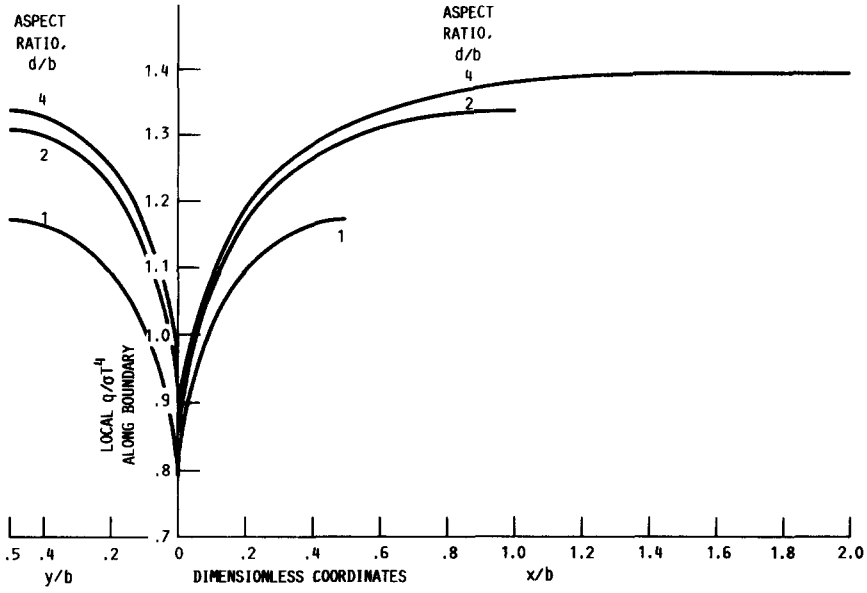

FIG. 6. Local values of the ratio $q/\sigma T^4$ along the boundary; optical dimension $ab = 2$.

results when the optical length of the short side is equal to 2 and 4. The results shown in Fig. 5 for a plane layer are also for fully developed transient cooling as obtained in ref. [7]. For rectangles with very large aspect ratios, the cooler end regions would become less important in determining the T_m value, and the curves of $q_\ell/\sigma T_m^4$ along the long side will then approach the plane layer results. This trend is shown, for example, by comparing the curves for aspect ratios 2 and 4 in Fig. 5(b).

When forming an emittance, the local heat flux from the sides of the rectangle could be normalized relative to the local boundary temperature rather than using T_m. The result is shown in Fig. 6 for an optical dimension $ab = 2$. Since the transient boundary temperatures are generally lower than the mean temperature, the ratio $q/\sigma T^4$ gives values that are larger than those in Fig. 5. This serves to further emphasize the fact that much of the energy leaving the boundary is radiated out from the interior of the medium where the temperatures are higher than at the boundary. This effect is accentuated as the optical density is increased, which increases the nonuniformity of the temperature distribution. To further examine this effect, the local heat flux at the center of the long side was divided by $\sigma T^4(d/2, b)$ on the boundary at that location. As shown in Fig. 7, this ratio increases as the optical dimension ab increases, and it also increases with the aspect ratio of the rectangle. When the aspect ratio approaches 4, this local ratio has almost reached the value for a plane layer.

Having discussed the local fluxes around the rectangle, the emittance for the total region is now examined as obtained from equation (19) using the local ε values from either equation (17) or equation (18). To compare rectangles having various aspect ratios with

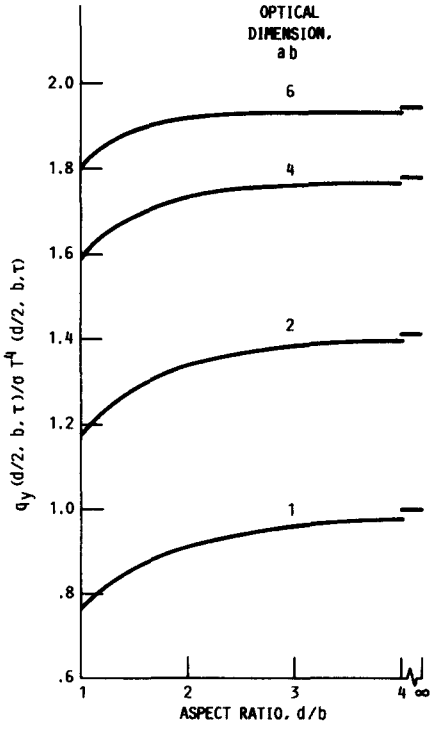

FIG. 7. Local emittance at center of long side of rectangle for fully developed transient cooling.

each other, and with a cylinder and a plane layer, it is convenient to use a characteristic optical dimension. The optical mean beam length $aL_{e,o}$ for an optically thin region is used as defined in equation (21). This causes all the average ε curves to come together when the regions are optically thin. Figure 8(a) shows the emittance for the rectangle at uniform temperature T_i.

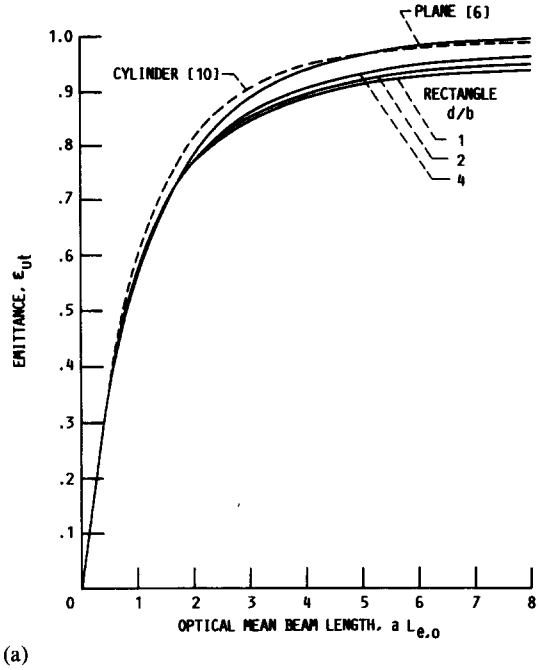

(a)

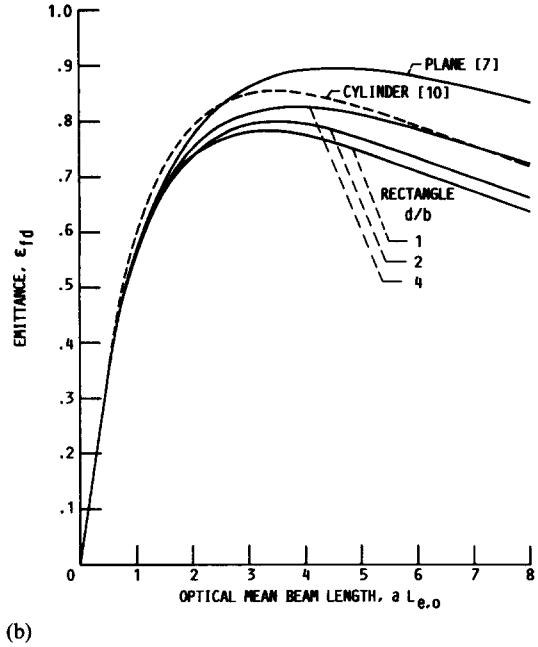

(b)

FIG. 8. Emittance for cooling a rectangular region compared with a plane region and a cylinder: (a) values for region at uniform temperature; (b) values for fully developed transient cooling.

Numerical values are given in Table 2. The heat loss per unit of length z is related to this emittance by $Q = 2\varepsilon_{ut}(b+d)\sigma T_i^4$. For a region with uniform temperature, the emittance increases continuously with $aL_{e,o}$, and when $aL_{e,o} = 8$, the cylinder and plane layer have become almost black. The rectangular shapes have somewhat lower emittance values as a result of the poor emissive ability in the corner regions. As the aspect ratio increases and the corner regions become proportionately less important, the ε_{ut} values for the rectangular shapes gradually approach the values for a plane layer.

Table 2. Area averaged emittance values for cooling of a rectangular region at uniform temperature and for fully developed transient conditions

Aspect ratio, d/b		Optical dimension, ab			
		1	2	4	6
1	ε_{ut}	0.570	0.767	0.887	0.926
	ε_{fd}	0.565	0.739	0.776	0.711
	F_m	1.041	1.076	1.135	1.187
2	ε_{ut}	0.656	0.832	0.925	0.948
	ε_{fd}	0.646	0.783	0.757	0.664
	F_m	1.040	1.075	1.140	1.197
4	ε_{ut}	0.708	0.874	0.951	0.966
	ε_{fd}	0.695	0.818	0.774	0.674
	F_m	1.040	1.081	1.156	1.223

The emittance values for fully developed transient cooling in low temperature surroundings are shown in Fig. 8(b). The heat loss per unit of length z for the rectangular regions is $Q = 2\varepsilon_{fd}(b+d)\sigma T_m^4$. As the optical mean beam length is increased, ε_{fd} passes through a maximum for each geometry and then decreases. The peak ε_{fd} are in the range of $aL_{e,o}$ from about 3 to 5. For a plane layer, the mean beam length is twice the layer thickness; so the peak is at an optical thickness of the layer of about 2.5. The decrease in emittance at larger thicknesses is because the outer regions have much lower temperatures than those in the interior. This provides a lower emissive ability compared with a region at uniform temperature.

CONCLUSIONS

The radiative ability of an emitting and absorbing rectangular region was analyzed to examine transient cooling behavior. The energy equation formulated with the radiative heat fluxes is a two-dimensional non-linear integral equation for the temperature distribution. This was solved numerically by iteration for various aspect ratios of the rectangular region and for various optical lengths of the smaller boundary. To solve the integral equation, the two-dimensional integrals in the energy exchange were evaluated with Gaussian integration subroutines. These integration procedures were also used to obtain the local surface heat fluxes after the temperature distribution was obtained. For conditions at the onset of transient cooling, when the region is still at uniform temperature, the average emittance for the rectangle is increased when the optical mean beam length of the region is increased. This behavior is compared with the fully developed transient results that were found

using a separation of variables solution for cooling in low temperature surroundings. For transient cooling, the emittance is decreased as the optical thickness becomes large. This is the result of the transient temperature distribution where the outer regions become much cooler than the interior. The average emittance values provide upper and lower bounds for the radiative performance during the transient cooling process. They show how significantly the transient behavior can deviate from that for radiation from a region at uniform temperature.

Acknowledgment—Mr Frank Molls of the Lewis Research Center provided considerable help in developing the computer program and testing its accuracy. His help is gratefully acknowledged.

REFERENCES

1. W. W. Yuen and L. W. Wong, Analysis of radiative equilibrium in a rectangular enclosure with gray medium, *J. Heat Transfer* **106,** 433–440 (1984).
2. M. M. Razzaque, J. R. Howell and D. E. Klein, Coupled radiative and conductive heat transfer in a two-dimensional rectangular enclosure with gray participating media using finite elements, *J. Heat Transfer* **106,** 613–619 (1984).
3. C. H. Ho and M. N. Ozisik, Combined conduction and radiation in a two-dimensional rectangular enclosure, *Numer. Heat Transfer* **13,** 229–239 (1988).
4. W. W. Yuen and C. F. Ho, Analysis of two-dimensional radiative heat transfer in a gray medium with internal heat generation, *Int. J. Heat Mass Transfer* **28,** 17–23 (1985).
5. W. A. Fiveland, Discrete-ordinates solutions of the radiative transport equation for rectangular enclosures, *J. Heat Transfer* **106,** 699–706 (1984).
6. R. Siegel, Transient radiative cooling of a droplet-filled layer, *J. Heat Transfer* **109,** 159–164 (1987).
7. R. Siegel, Separation of variables solution for non-linear radiative cooling, *Int. J. Heat Mass Transfer* **30,** 959–965 (1987).
8. R. Siegel and J. R. Howell, *Thermal Radiation Heat Transfer* (2nd Edn), pp. 458 and 616. Hemisphere, Washington, DC (1981).
9. W. W. Yuen and L. W. Wong, Numerical computation of an important integral function in two-dimensional radiative transfer, *J. Quant. Spectrosc. Radiat. Transfer* **29,** 145–149 (1983).
10. R. Siegel, Transient radiative cooling of an absorbing and scattering cylinder—a separable solution, *J. Thermophys. Heat Transfer* **2,** 110–117 (1988).

QUELQUES ASPECTS DU REFROIDISSEMENT VARIABLE D'UN MILIEU RECTANGULAIRE RADIANT

Résumé—L'emission d'un milieu gris rayonnant est analysé pour le refroidissement variable dans des ambiances à basse température. Le milieu est rectangulaire, sans variation dans la direction normale à la section droite. L'équation intégrale pour la distribution variable de température est résolue numériquement en utilisant une méthode d'intégration gaussienne à deux dimensions. L'émission pour un rectangle à température uniforme est comparée à celle pour un refroidissement où la distribution de température a atteint une forme pleinement établie, comme le montre une solution par séparation des variables. Les deux solutions fournissent les limites supérieure et inférieure de l'émittance d'un rectangle pendant le refroidissement variable. Les émittances pour plusieurs rapports de forme sont présentés en fonction de la longueur du rayon moyen et sont comparés avec des résultats pour une couche plane et un cylindre.

INSTATIONÄRES ABKÜHLEN EINES STRAHLENDEN RECHTECKIGEN KÖRPERS

Zusammenfassung—Es wird die Emission eines grau strahlenden Körpers untersucht, der sich in einer Umgebung von geringer Temperatur abkühlt. Die Grundfläche des Körpers ist rechteckförmig, die Dicke überall konstant. Die Integral-Gleichung für die instationäre Temperaturverteilung wird mit Hilfe eines Integrations-Unterprograms für zweidimensionale Fälle nach Gauss numerisch gelöst. Die Emissivität eines Rechtecks bei konstanter Temperatur wird verglichen mit der Emissivität beim instationären Abkühlvorgang, wobei das Temperaturfeld als voll ausgebildet angenommen wird. Die beiden Lösungen stellen die obere und untere Grenze für die Abstrahlung eines Rechtecks während des instationären Abkühlvorgangs dar. Die Abstrahlung wird für verschiedene Seitenverhältnisse dargestellt und mit den Ergebnissen für eine ebene Schicht und einen Zylinder verglichen.

НЕКОТОРЫЕ АСПЕКТЫ НЕСТАЦИОНАРНОГО ОХЛАЖДЕНИЯ ИЗЛУЧАЮЩЕЙ СРЕДЫ ПРЯМОУГОЛЬНОЙ ФОРМЫ

Аннотация—Анализируется эмиссия от серой излучающей среды в случае охлаждения в нестационарном режиме при низкой температуре охлаждающей среды. Излучающая среда имеет прямоугольную форму, не изменяющуюся в направлении, перпендикулерном поперечному сечению. Интегральное уравнение для нестационарного распределения температцры решается численно с использованием метода Гаусса для расчета интегралов. Сравнивается излучательная способность прямоугольника при постоянной температуре и при охлаждении в нестационарном режиме в случае полностью развитого распределения температцр, полученного методом разделения переменных. Указанные решения определяют верхнюю и нижнюю границы изучения прямоугольника при нестационарном охлаждении. Излучательная способность для различных значений отношения сторон представлены как функция средней луча прямоугольника и сравниваются с резульатами для плоского слоя и цилиндра.